Applied Organometallic Chemistry **WILEY**

Novel palladium nanoparticles supported on mesoporous natural phosphate: Catalytic ability for the preparation of aromatic hydrocarbons from natural terpenes

Ayoub Abdelkader Mekkaoui[1,2] ⬤ | **Abderrazak Aberkouks**[2] | **Lahcen Fkhar**[2] | **Mustapha Ait Ali**[2] | **Larbi El Firdoussi**[2] | **Soufiane El Houssame**[1] ⬤

[1]Laboratoire de Chimie, Modélisation et Sciences de l'environnement, Université Sultan Moulay Slimane, Faculté Polydisciplinaire de Khouribga, B. P 145, Khouribga, 25000, Morocco

[2]Département de Chimie, Faculté des Sciences Semlalia, Laboratoire de chimie de Coordination et de Catalyse, 2390, Marrakech, BP, 40001, Morocco

Correspondence
Ayoub Abdelkader Mekkaoui, Laboratoire de chimie de Coordination et de Catalyse, Département de Chimie, Faculté des Sciences Semlalia. BP 2390, 40001 Marrakech, Morocco.
Email: mekk.ayoub@gamil.com

Soufiane El Houssame, Laboratoire de Chimie, Modélisation et Sciences de l'environnement, Université Sultan Moulay Slimane, Faculté Polydisciplinaire de Khouribga, B. P 145, 25000. Khouribga, Morocco.
Email: hous_soufiane@hotmail.com

Various ratios of palladium nanoparticles supported on mesoporous natural phosphate (Pd@NP) were prepared using the wetness impregnation method. The prepared catalysts were characterized by IR, XRD, CV, SEM, EDX, XRF, TEM and BET analysis. The reduction and preparation of the palladium nanoparticles afford a crystallite size of 10.88 nm. The performance of the synthesized catalyst was investigated in the solvent-free dehydroaromatization of α-, β- and γ-himachalene mixture from Cedrus atlantica oil as a model substrate. In order to achieve an efficient and selective catalysis, the catalytic dehydroaromatization of various terpenes such as limonene, limonaketone, carvone, carveol and perillyl alcohol was studied. The Pd@NP catalyst performed a high catalytic activity, selectivity and recyclability in the terpenes dehydroaromatization reaction.

KEYWORDS

dehydroaromatization, heterogeneous catalysis, mesoporous natural phosphate, palladium nanoparticles, terpenes

1 | INTRODUCTION

The use of naturally occurring materials as heterogeneous catalysts or catalytic carriers has experienced rapid progress in recent years, as recycling and low cost are extremely important from both an industrial and environmental perspective.[1–4] They have been presented as renewable raw materials for producing biofuels and useful products through green processes that are very important in the context of sustainable development and circular economy.

Away from the various used supported catalysts, only a few works are devoted to natural phosphate (NP) as support.[5–7] Furthermore, solid phosphates such as NP, fluorapatite or hydroxyapatite have been prepared and used as catalysts.[7–10] To the best of our knowledge, NP has been used for the first time as a support for metal nanoparticles.[7] Due to the important feature of mesoporous materials that allows a high distribution of active centers, mesoporous NP provides a high distribution and dispersion of palladium nanoparticles.[7] Relying on NP is the first mining industry in the Moroccan kingdom, as a natural and low-cost material that exhibits interesting properties, such as ionic substitution ability, structural stability and high adsorption capacity, making it an attractive and cost-effective catalyst or catalytic carrier for several chemical transformations.

Scientists are giving more focus on the use of readily available and relatively cheap compounds of natural origin. This trend is perfectly suited with the design of a clean process to transform terpenes, renewable raw materials into aromatic derivatives value-added products usually prepared from non-renewable fossil resources, i.e. paracymene prepared by alkylation of benzene or toluene.[11] Therefore, the catalytic dehydroaromatization presents a sustainable and economical alternative to selective aromatic terpenes starting from naturally occurring terpenes.

Atlas Cedar or Cedarwood (*Cedrus atlantica*) belonging to the family of Pinaceae is the principal species in Moroccan forests, its oil consists of several products such as insecticides, drugs, perfumes, etc.[12–16] Ar-himachalene is an important intermediate in industrial fine chemical synthesis of fragrances,[13,17] and the male-produced pheromone component of the flea beetles *Aphthona flava* and *Phyllotreta cruciferae*.[18,19] Moreover, the aromatization of himachalenes derivatives slightly increased the antibacterial activity, and confirmed that ar-himachalene is widely represented in natural products and pharmaceuticals.[20,21] Due to its benefits, various studies have been reported on the synthesis of ar-himachalene either by total synthesis or by dehydroaromatization of himachalene derivatives.[19–32] Different dehydroaromatization agents were used, such as: lithium,[29] selenium,[28,30] chloranile,[23] Pd/C,[20,24] Raney nickel,[31] bromine[32] or DDQ (2,3-dichloro-5,6-dicyano-1,4-benzoquinone).[20]

It is noteworthy that different works are reported for the p-cymene preparation in the presence of various dipentene derivatives, such as carene, pinene or limonene.[33–37] The conversion of limonene, a cheap by-product of the citrus industry, into p-cymene represents a promising green route.[38–46] Catalysts providing acid

sites for isomerization-disproportionation and metallic sites for subsequent dehydroaromatization are more suitable.[40,41,47] Amongst the used metallic catalysts, palladium has been demonstrated as the active center for limonene dehydrogenation.[47–53] While heterogeneous acid catalysts such as zeolites have been widely used, the reaction is affected with the formation of by-products.[54–58]

Herein, our attention focused on the preparation, characterization and catalytic dehydroaromatization of various palladium nanoparticles supported NP (Pd@NP 1%, 5% and 10%). To extend the scope of the catalytic application, functionalized terpenes such as limonaketone, carveol and perillyl alcohol were chosen for the first time as exclusive substrates for dehydroaromatization. The prepared nanocatalysts represent a good choice for dehydroaromatization product selectivity under solvent-free conditions. To the best of our knowledge, a relevant study is missing, which leads us to believe that this method using mild conditions may represent a valuable alternative to the existing procedures in order to replace the present petroleum-based source of most of the aromatic hydrocarbons industry.

2 | EXPERIMENTAL

2.1 | Catalyst preparation

2.2 | Mesoporous natural phosphate support

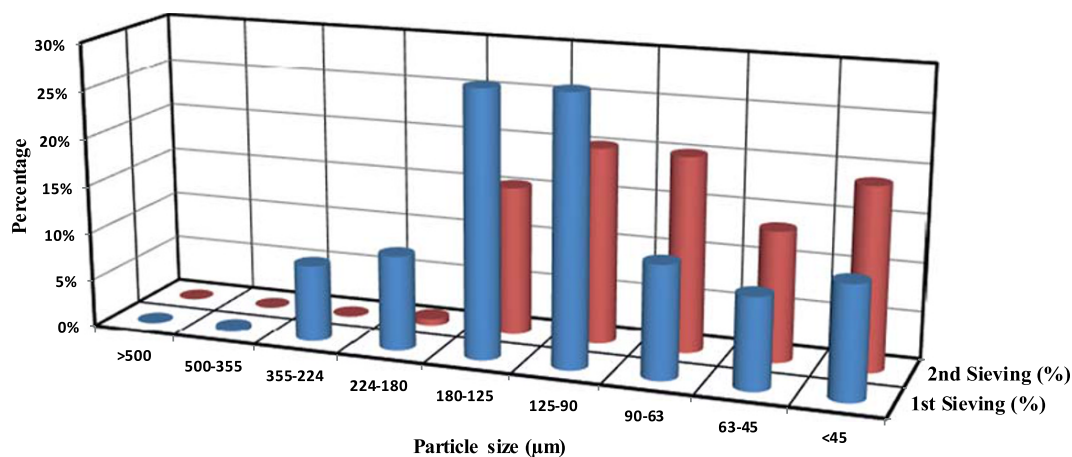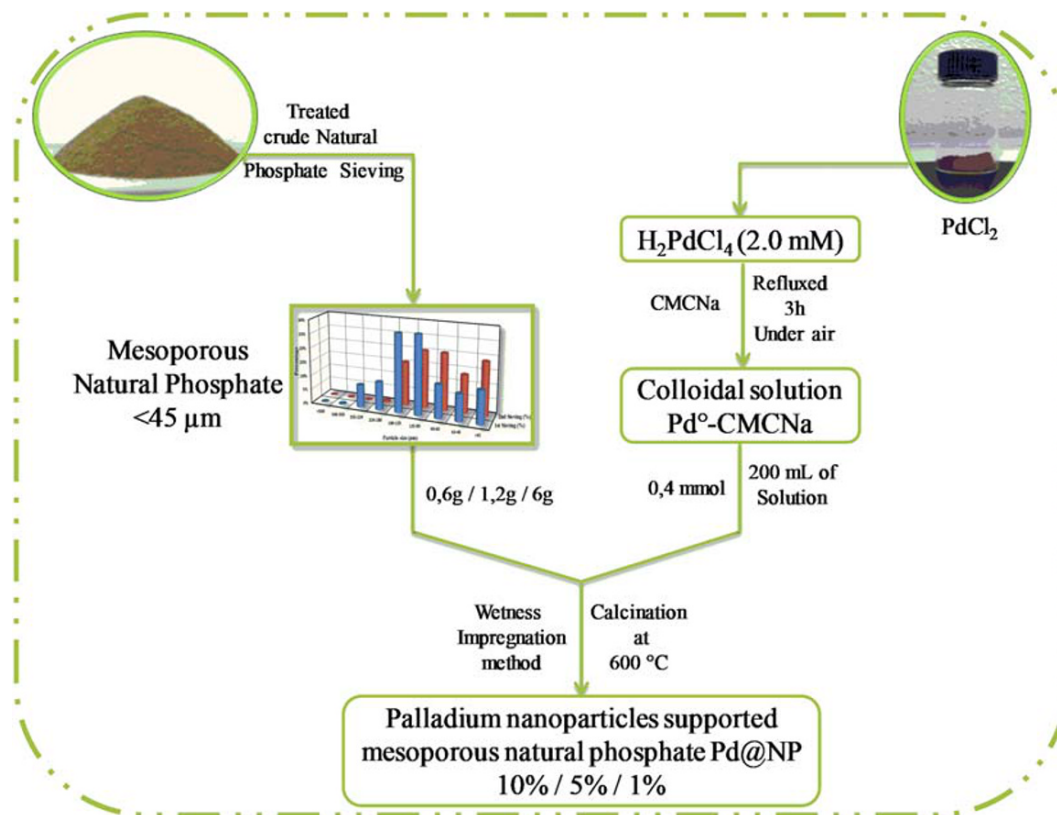The used NP was obtained from 'Khouribga' region (Morocco).[59] After being treated using several

**FIGURE 1** Particle size distribution after first and second sieving

SCHEME 1 Method of Pd@NP catalysts (10%, 5% and 1%) synthesis

techniques, involving attrition, sifting, calcinations (900°C), washing and re-calcination, its chemical composition was found to be: CaO (54.12%), P_2O_5 (34.24%), F (3.37%), SiO_2 (2.42%), SO_3 (2.21%), CO_2 (1.13%), Na_2O (0.92%), MgO (0.68%), Al_2O_3 (0.46%),

Fe_2O_3 (0.36%), K_2O (0.04%) and several metals in the range of ppm.

Prior to use, homogeneous mesoporous NP support with particle size of < 45 μm was prepared by grinding and sieving several times (Figure 1).
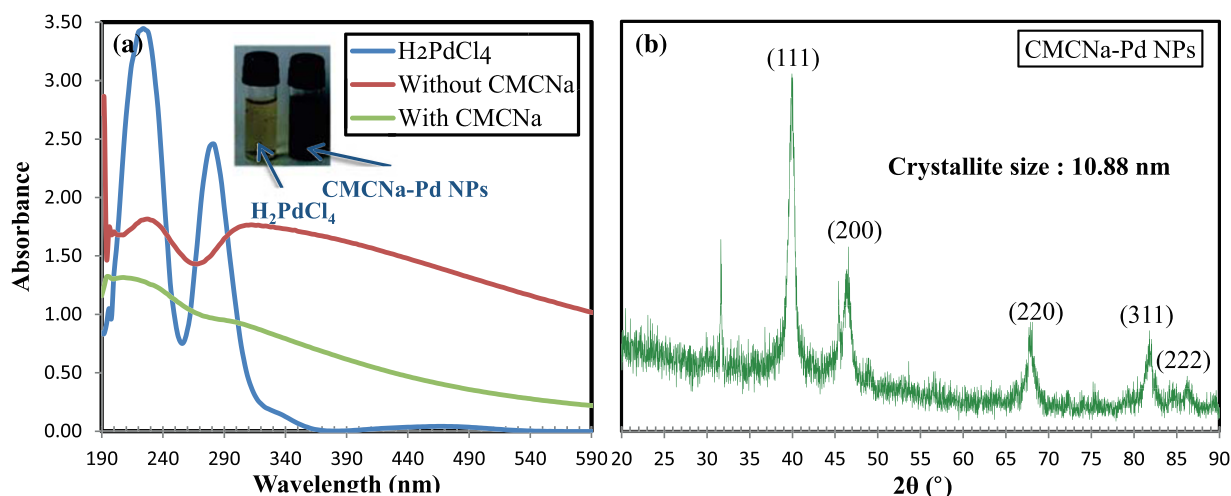
FIGURE 2 (a) UV–Vis spectra of H_2PdCl_4 reduction with and without CMCNa; and (b) X-ray diffraction (XRD) pattern of the as synthesized CMCNa-Pd nanoparticles

## 2.3 | Colloidal solution of palladium nanoparticles

The colloidal solution of palladium nanoparticles was prepared as described previously.[7] An aqueous solution of H_2PdCl_4 (200 ml, 2.0 mM) was added to 70 ml of water, 47 ml of ethanol and 0.22 g of sodium carboxymethylcellulose (CMC-Na). The mixture was refluxed for 3 hr under air. The palladium nanoparticles preparation was followed up by UV–Vis spectroscopy. The resulting monodispersed palladium nanoparticles were used for the preparation of different Pd@NP catalysts (10%, 5% and 1%).

2.4 | Deposition of Pd (0) metal nanoparticles on mesoporous natural phosphate

A solution of 200 ml of the prepared Pd (0) nanoparticles (0.4 mmol) was added to 0.6, 1.2 and 6 g of the mesoporous NP to prepare Pd@NP catalyst 1%, 5% and 10%, respectively. The catalysts were synthesized by wetness impregnation for 24 hr followed by calcination in a tube furnace at 600°C for 3 hr (Scheme 1).

3 | CATALYST CHARACTERIZATION

Spectrophotometric analysis was investigated using a double-beam scanning spectrophotometer (Shimadzu spectrophotometer, model biochrom). Fourier transform-infrared (FT-IR) transmittance spectra were recorded in the region of 400–4000 cm^{-1} using a FT-IR spectroscopy
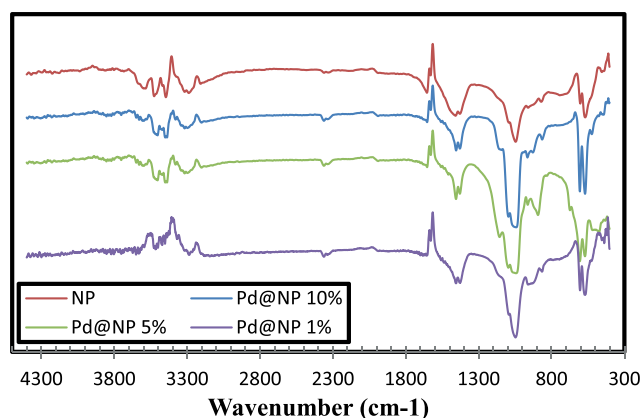

FIGURE 3 Fourier transform-infrared (FT-IR) spectrum of pure NP and Pd@NP (1%, 5% and 10%)

model Perkin Elmer (FTIR-2000). Diffraction data were collected at room temperature on a D2 PHASER diffractometer (BRUKER-AXS), with the Bragg–Brentano geometry, using CuKα radiation ($\lambda = 1.5406$ Å) with 30 kV and 10 mA. The patterns were scanned through steps of 0.010142 (2θ) in the 2θ range 5–70°. Cyclic voltammetry (CV) study was performed between 1500 mV/−500 mV and 1200 mV/300 mV for carbon paste electrode (CPE) modified by our samples in 0.5 M H_2SO_4 electrolyte at scan rate 100 mV/s using PGZ 100 potentiostat in the presence of platinum auxiliary electrode and Ag/AgCl (KCl 3 M) reference electrode. Textural characteristics of the prepared samples such as Brunauer−Emmett−Teller (BET) surface area and average pore diameter were determined by N_2 adsorption–desorption technique using Micromeritics 3FLEX analyzer. Prior to measurements, all samples were degassed at 120°C during 12 hr under vacuum. Scanning electron microscopy (SEM) measurements were obtained with TESCAN VEGA3-EDAX equipped with an energy-
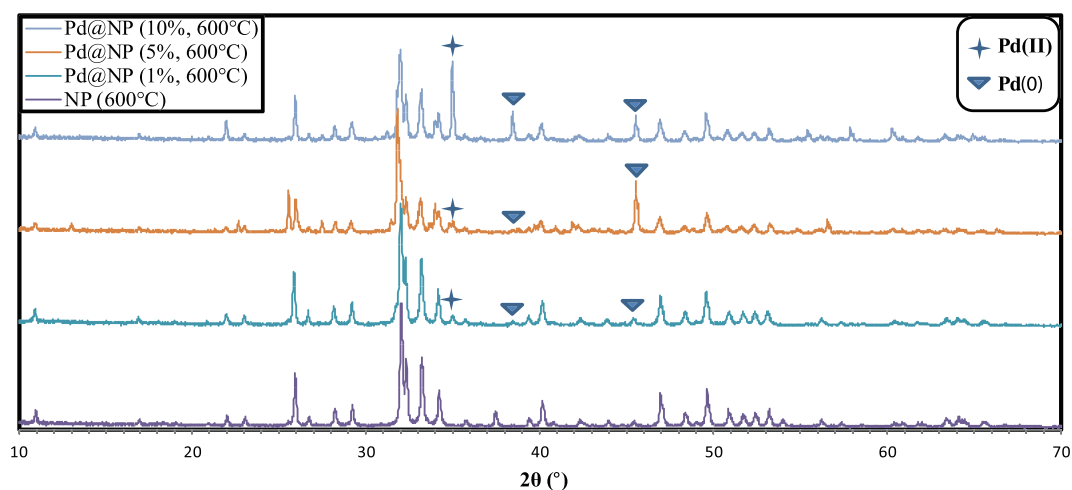
**FIGURE 4** X-ray diffraction (XRD) patterns of NP and Pd@NP (10%, 5% and 1%) calcined at 600°C

FIGURE 5 Cyclic voltammetry (CVs) of carbon paste electrode (CPE) modified by $PdCl_2$ and Pd@NP (10%, 5% and 1%) performed between: (a) 1500 mV/−500 mV and (b) 1200 mV/300 mV at scan rate 100 mV/s
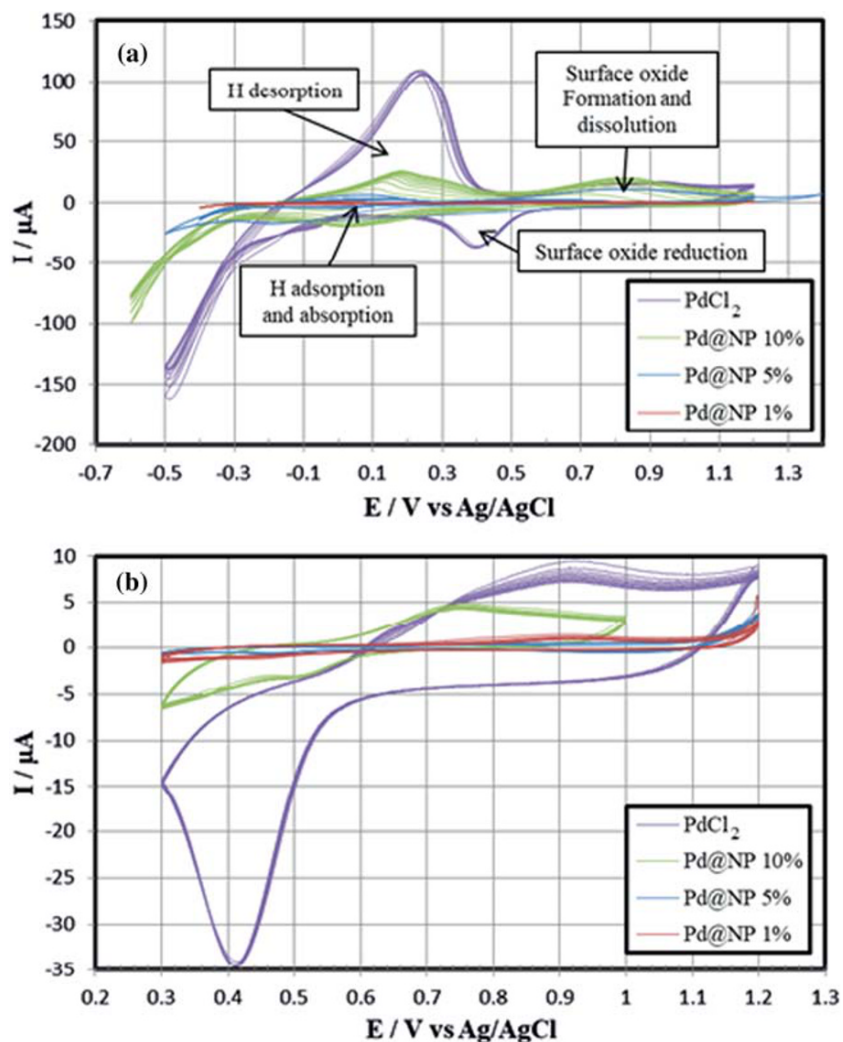
dispersive X-ray detector (EDX). Transmission electron microscopy (TEM) observations were carried out at 100 kV (JEOL 1200 EXII). Samples were prepared by embedding the hybrid material in AGAR 100 resin, followed by ultramicrotomy techniques and deposition on copper grids.

4 | GENERAL PROCEDURE FOR THE SOLVENT-FREE CATALYTIC DEHYDROAROMATIZATION

The prepared nanocatalysts Pd@NP (1%, 5% and 10%) were studied over a solvent-free dehydroaromatization.
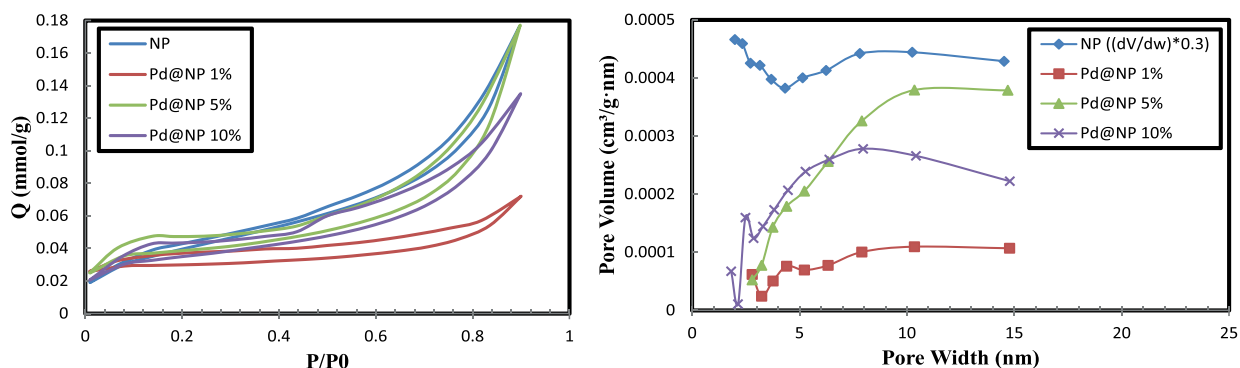
FIGURE 6 Nitrogen adsorption isotherm and pore diameter distribution of NP and Pd@NP catalysts (1%, 5% and 10%) calcined at 600°C

The reaction was carried out in the presence of Pd@NP and the freshly distilled natural α-, β- and γ-himachalene mixture, i.e. the main components of *Cedrus atlantica* oil, which together can make up almost 70% of the composition. The mixture was refluxed in a solvent-free media for 24 hr. The scope and limitation of the catalytic system were examined by testing various parameters, such as: catalyst amount, reaction time and catalyst recyclability. Under the optimized conditions, the dehydroaromatization of various monoterpenes [limonene, natural limonaketone (distilled from *Cedrus atlantica* oil), carvone, carveol and perillyl alcohol] was studied. The reaction process was monitored by Shimadzu gas chromatography (GC) equipped with FID using Rtx-5 capillary column (25 m × 0.25 mm) and nitrogen as a carrier gas. Dodecane was used as an internal standard for the quantitative analysis of the reaction products. The GC parameters are: injector 250°C; detector 250°C; oven 70°C for 5 min then 3°C/min until 250°C for 30 min; column pressure 20 kPa, column flow 6.3 ml/min; linear velocity 53.1 cm/s; total flow 138 ml/min. All products were confirmed by injecting the reaction mixture on an ISQ LT single quadrupole mass spectrometer in positive EI mode using a mass scan range of 50−400 Da. Isolated products were subjected to NMR and GC–MS analysis.

5 | RESULTS AND DISCUSSION

6 | CATALYST CHARACTERIZATION

6.1 | Colloidal solution of palladium nanoparticles

UV–Vis spectra (Figure 2) of H_2PdCl_4 solution before and after reduction (with and without CMC-Na) confirms that the transition-metal precursor H_2PdCl_4 was totally reduced to nano-Pd (0).[7] Previously, we have demonstrated that the crystallinity of the as-synthesized face centered cubic (fcc) structure of palladium nanoparticles (CMCNa-Pd NPs) was examined by X-ray diffraction (XRD) analysis with an average crystallite size of 10.88 nm (Figure 2).[7]

6.2 | Palladium nanoparticles supported on natural phosphate (Pd@NP)

The prepared colloidal solution was used to synthesize the palladium nanoparticles-supported mesoporous NP catalysts using the wetness impregnation method followed by calcination at 600°C.

FT-IR spectra (Figure 3) of NP and Pd@NP catalysts (1%, 5% and 10%) showed for both samples many characteristic bands of crystalline apatite (phosphate groups at 470, 560–600, 960, 1030–1120 cm^{-1}).[60]

Recently, we have shown different XRD patterns of the prepared Pd@NP 10% compared with the literature due to the presence of palladium over the mesoporous NP.[7] Consequently, Pd@NP catalysts (1%, 5% and 10%) showed the same result (Figure 4), and two oxidation states Pd (0) and Pd (II) were observed. The presence of Pd (II) is due to re-oxidation of Pd (0) during the calcination. Depending on the intensity of Pd (II) pics, the prepared Pd@NP 1% and 5% showed a noticeable difference compared with Pd@NP 10%, which confirms that re-oxidation of Pd (0) during calcination is neglected for palladium catalyst content less than 10%. Consequently, we can assume that oxidation of Pd (0) in low content materials could be avoided without excluding oxygen.

The CV experiments represent a good alternative for the determination of the metal predominant oxidation state.[7,61] A study of the prepared palladium species supported over the NP ($PdCl_2$ and Pd@NP 1%, 5% and 10%) was carried out (Figure 5).

Previously, we confirmed the predominance of Pd (0) compared with Pd (II) by a comparison of Pd@NP 10% (before and after calcination) and $PdCl_2$ voltammograms.[7] The study of the surface oxide zones of all prepared catalysts (Pd@NP 1%, 5% and 10%) confirms the results of Pd (0) predominance (Figure 5). On the other hand, the hydrogen zones (Figure 5b) demonstrate the efficiency of the prepared catalyst and the importance of palladium over the mesoporous NP for

TABLE 1 BET surface area, average pore diameter and pore volume of NP and Pd@NP catalysts (1%, 5% and 10%)

Sample	BET surface area (m²/g)	BET average pore diameter (nm)	Pore volume (cm³/g)
NP	14.893	7.327	2.728*10^{-2}
Pd@NP 1%	2.082	4.806	2.502*10^{-3}
Pd@NP 5%	2.821	8.731	6.185*10^{-3}
Pd@NP 10%	3.754	7.236	6.792*10^{-3}

BET, Brunauer−Emmett−Teller.
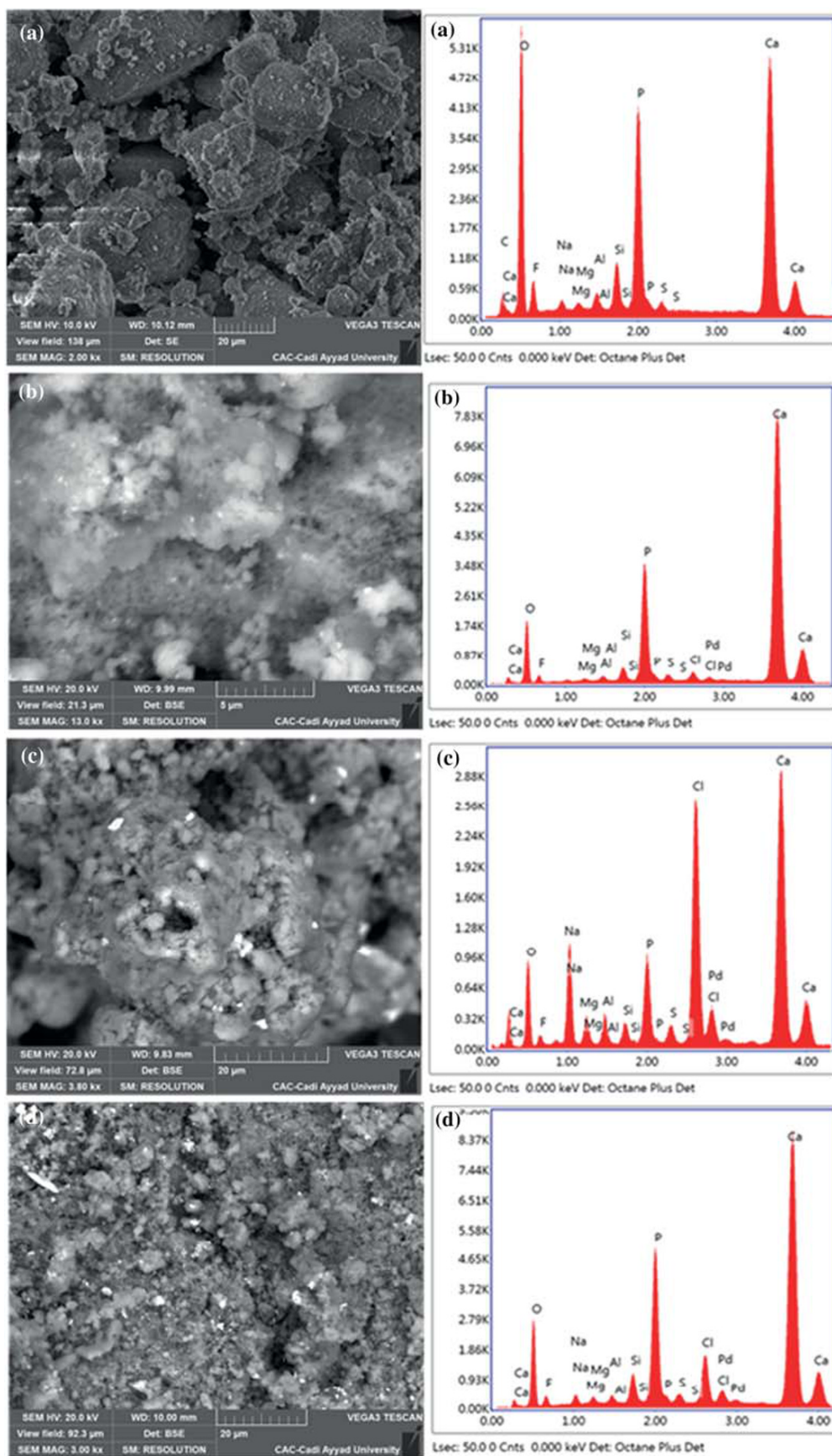
FIGURE 7 Scanning electron microscopy (SEM) images and energy-dispersive X-ray (EDX) analysis of: (a) NP and (b, c and d) Pd@NP (1%, 5% and 10%)

hydrogen transfer at the catalysts interface (NP was inert in the CV study compared with the other samples).

The BET measurements of NP and the prepared catalysts Pd@NP (1%, 5% and 10%) are reported in Figure 6 and Table 1. The BET surface area values of NP and Pd@NP 1%, 5% and 10% were, respectively, 14.893, 2.082, 2.821 and 3.754 m^2/g. Consequently, the decrease of S_{BET} of all prepared Pd@NP catalysts is caused by the deposition of Pd nanoparticles and the agglomeration of metal species during calcination. Furthermore, the average pore diameter and the pore volume confirm that the support and the catalysts are mesoporous materials.

The SEM images of the mesoporous NP and the prepared Pd@NP (1%, 5% and 10%) calcined at 600°C show that the surface morphology of the catalyst is not identical to that of NP support (Figure 7). All the prepared Pd@NP catalysts show the presence of Pd

(0) in nanoscale with good distribution, and present good dispersion of Pd species that were proportional to the Pd content over NP support. The EDX results of NP indicate the presence of all elements of fluorapatite structure in the mesoporous NP. The EDX of Pd@NP catalysts (1%, 5% and 10%) confirmed the presence of palladium and the fluorapatite composition remains unchanged.

Element distribution in the hybrid has been carried out for the prepared catalysts Pd@NP (1%, 5% and 10%; Figure 8). The main elements representing the NP [fluorapatite ($Ca_5(PO_4)_3F$) and other elements] showed a good distribution. Consequently, the same elements allow a good dispersion and distribution of palladium nanoparticles for all prepared Pd@NP catalysts (1%, 5% and 10%; Figure 8a−c).

The TEM study of NP and Pd@NP catalysts was also carried out (Figures 9 and 10). Mesoporous NP reveals
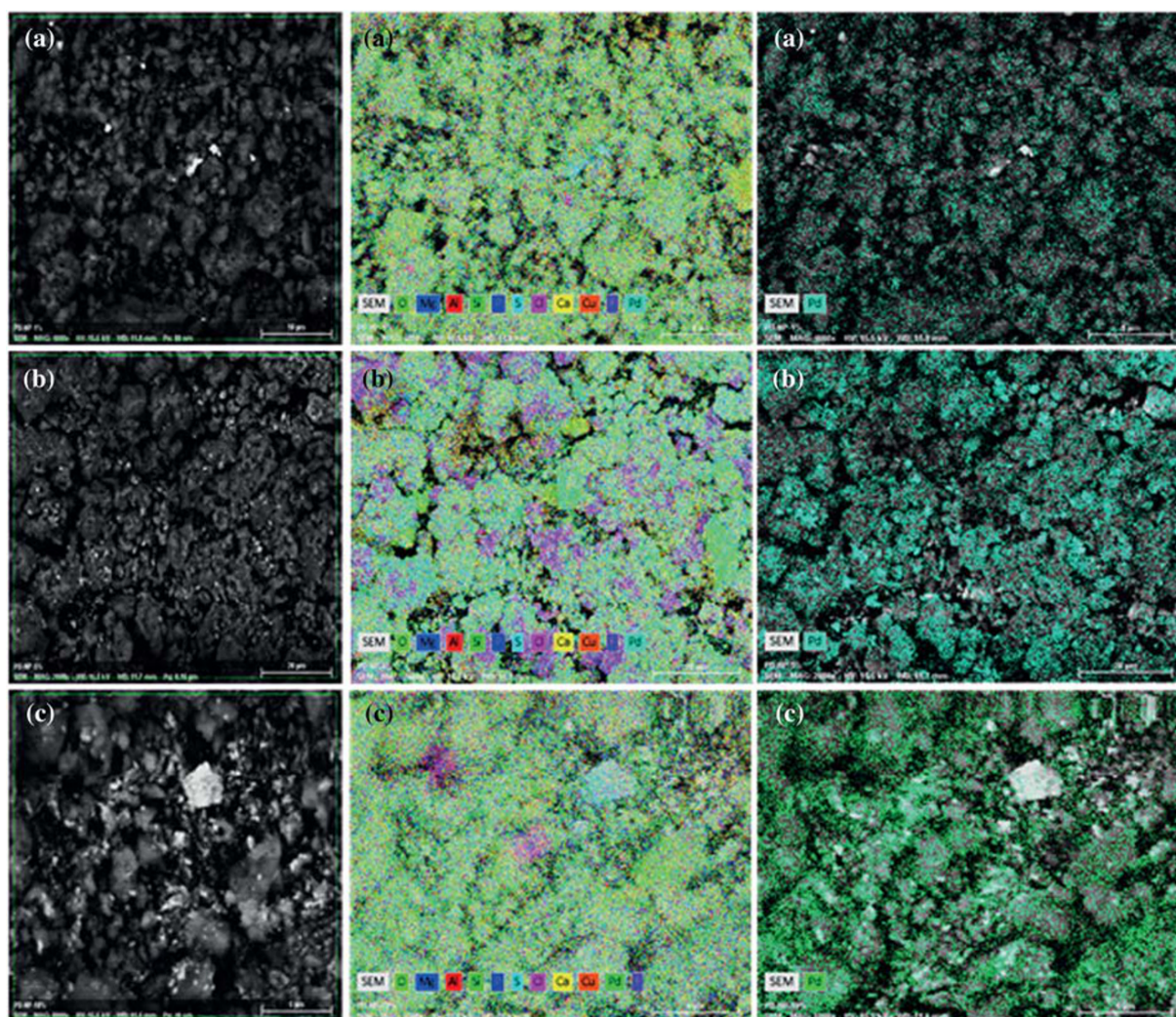
FIGURE 8 Energy-dispersive X-ray (EDX) elemental mapping analysis of: (a) Pd@NP 1%; (b) Pd@NP 5%; and (c) Pd@NP 10%
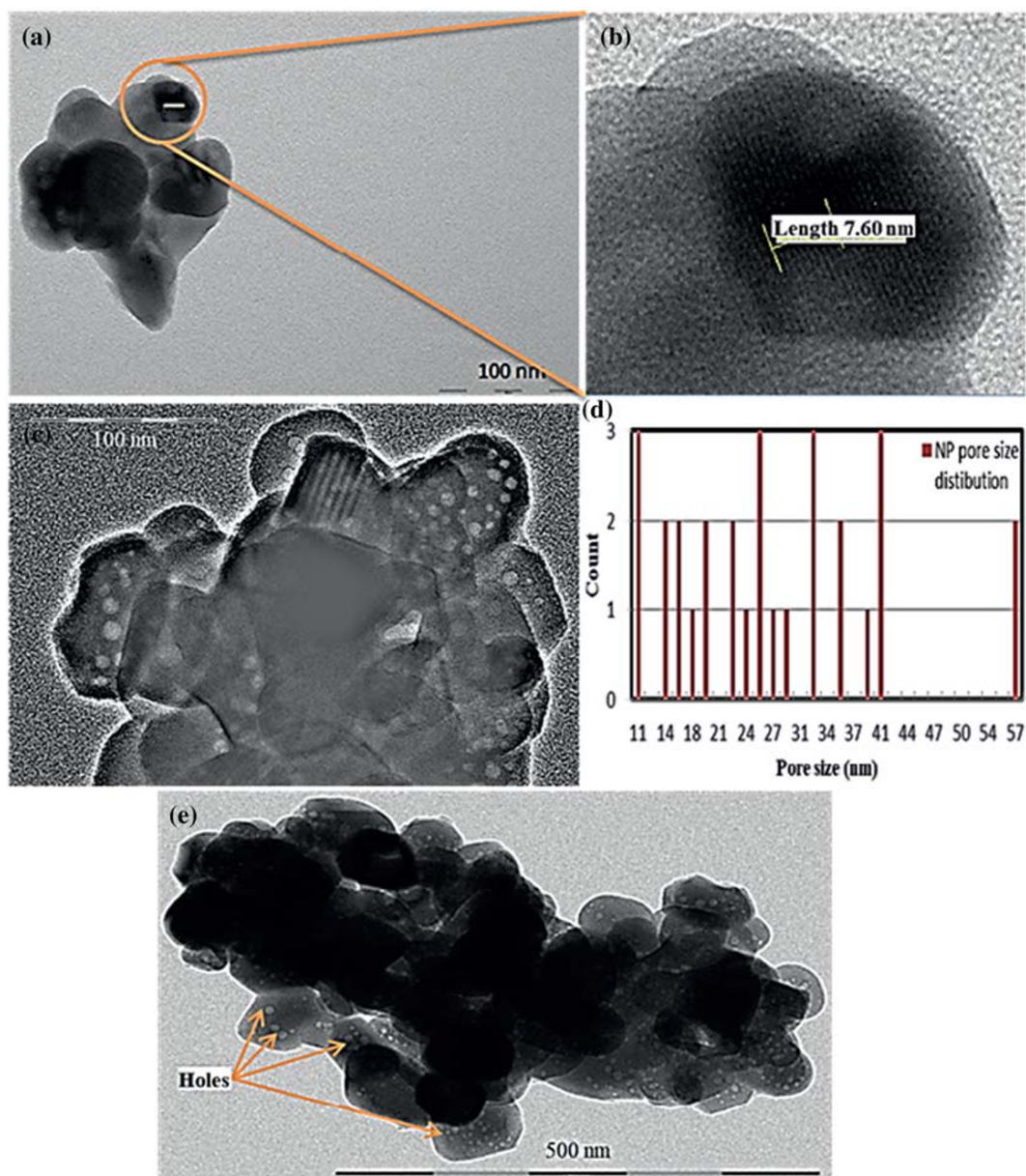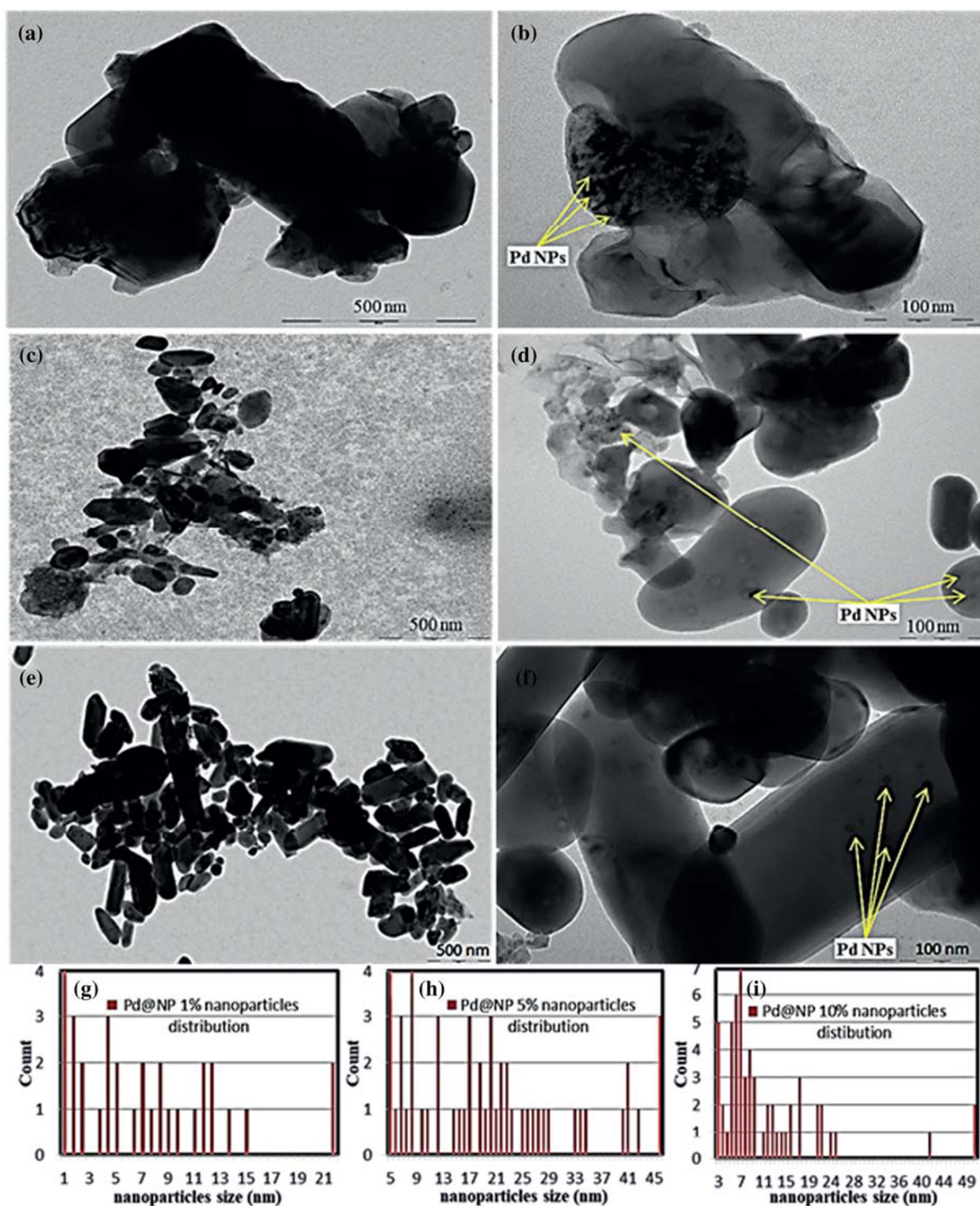
FIGURE 9 Transmission electron microscopy (TEM) images of NP with pore size distribution

irregular sphere-like particles (i.e. length/diameter) and agglomerated superstructures (Figure 9). This was consistent with the crystal size calculation according to XRD analysis, which indicated that the crystallite size of NP was found to be 63 nm. TEM images of NP present approximately the same particle sizes compared with those of synthetic ones.[62] Moreover, Figure 9 (a and b) reveals a lamellar aspect with a lamella size less than 1 nm. On the other hand, the analysis showed round bright patches (holes) distributed randomly in all the particles (Figure 9c and e) with a mean pore size of 28 nm (Figure 9d), explaining the

large surface area obtained by BET analysis compared with the prepared catalysts.

The TEM study of the prepared Pd@NP catalysts (1%, 5% and 10%) presents a slight difference in terms of morphology compared with NP (Figure 10). All samples reveal a different aspect of nano-sized grain crystals consistent with well-defined rod-like particles (Figure 10a, c and e). Furthermore, XRD crystal size calculation indicated that the Pd@NP catalysts (1%, 5% and 10%) crystallite sizes were found to be 67, 52 and 58 nm, respectively. The difference in shape between NP and Pd@NP catalysts can result in the

FIGURE 10 Transmission electron microscopy (TEM) images of Pd@NP catalysts with pore size distribution

preparation procedure (presence of CMC-Na during the impregnation). The distribution and deposition of the Pd nanoparticles were in a well-defined nanosphere shape (Figure 10 b, d and f), and the mean sizes of Pd@NP 1%, 5% and 10% were 7.60, 20.42 and 11.81 nm, respectively (Figure 10g−i).

The X-ray fluorescence (XRF) measurements of palladium in the prepared Pd@NP catalysts 10%, 5% and 1% were found to be 4.028%, 3.523% and 0.991%, respectively (Table 2).

The analysis results of all prepared Pd@NP catalysts (10%, 5% and 1%) confirm the good choice of the

TABLE 2 Palladium content in the Pd@NP catalysts by XRF analysis

Sample	Palladium (%)
Pd@NP 1%	0.991
Pd@NP 5%	3.523
Pd@NP 10%	4.028
Pd@NP 5% recycled	3.479
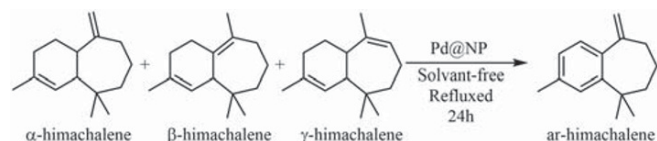
SCHEME 2 Dehydroaromatization of himachalene mixture over Pd@NP catalysts

palladium nanoparticles wetness impregnation as a simple advantageous method resulting particularly in a good distribution and dispersion of Pd compared with previous works.[5,6]

7 | CATALYTIC SOLVENT-FREE DEHYDROAROMATIZATION

The catalytic ability of the Pd@NP nanoparticles catalysts (10%, 5% and 1%) was evaluated for solvent-free dehydroaromatization of the natural mixture α-, β-and γ-himachalene chosen as a model substrate. The mixture was refluxed in the presence of the prepared catalysts for 24 hr (Scheme 2). In the presence of mesoporous NP support as catalyst, no dehydroaromatization was observed.

We have studied the effects of palladium content catalyst, catalyst amount and reaction time on the dehydroaromatization reaction (Figure 11a and b). Under optimized conditions, all the prepared catalysts show a high activity.

The catalyst/substrate (C/S: 5% weight) ratio was the best optimum amount for the catalytic application in the presence of Pd@NP 10% and Pd@NP 5%. However, Pd@NP 1% catalyst presents C/S = 10% (weight) as the optimum (Figure 11a).
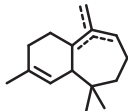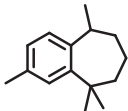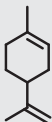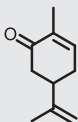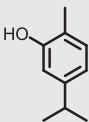
The effect of reaction time on catalytic activity is shown in Figure (11b). The catalytic dehydroaromatization reaction was faster in the first 2 hr, and a maximum of ar-himachalene was reached after 24 hr.

Under the optimized conditions, catalytic solvent-free dehydroaromatization of various terpenic olefins has been carried out (Table 3). As shown in Table 3, all terpenes were converted to the aromatic product in good yields (Entries 1–6).
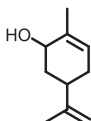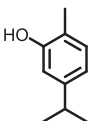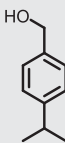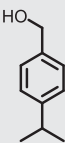
The reusability of Pd@NP 5% catalyst was carried out in the dehydroaromatization of himachalene mixture as a substrate. The catalytic performance was evaluated in six consecutive runs (Figure 12). The catalyst exhibited a high activity over the six runs, which improved the stability of the catalytic performance (Figure 12a). After the last run, the identity of the recovered catalyst was checked by XRD analysis (Figure 12b), which shows that the crystallinity remains similar after six runs with a slight difference
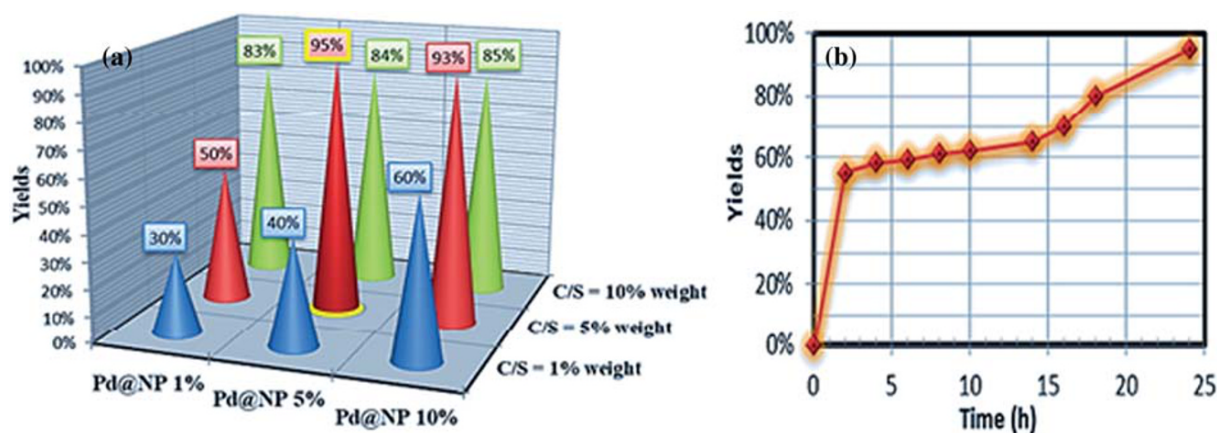
FIGURE 11 Optimization study of the catalytic dehydroaromatization: (a) palladium content catalysts and catalyst amount effect; and (b) reaction time

**TABLE 3** Pd@NP catalytic performance for solvent-free dehydroaromatization of various terpenes[a]

Entry	Substrate	Product	Conversion[b] (%)	Isolated yield (%)
1			99%	95%
2			90%	88%
3			81%	80%
4			95%	94%
5			99%	90%
6			99%	91%

[a]Reaction conditions: substrate and 5% weight of Pd@NP 5% refluxed for 24 hr in solvent-free conditions.
[b]Conversion was determined by GC using dodecane as an internal standard.

in peak intensity. In addition, the XRF study confirms that the palladium leaching is neglected even after six runs (Table 2). SEM images showed a stable morphology and relatively dispersed nanoparticles even after six runs (Figure 13a). Moreover, EDX indicated the composition stability of the prepared catalyst (Figure 13b). However, EDX elemental distribution of the recovered catalyst confirmed the composition stability (Figure 13d), and indicated that Pd nanoparticles remain stable in terms of distribution with a slight difference in dispersion compared with the fresh one (Figure 13e).
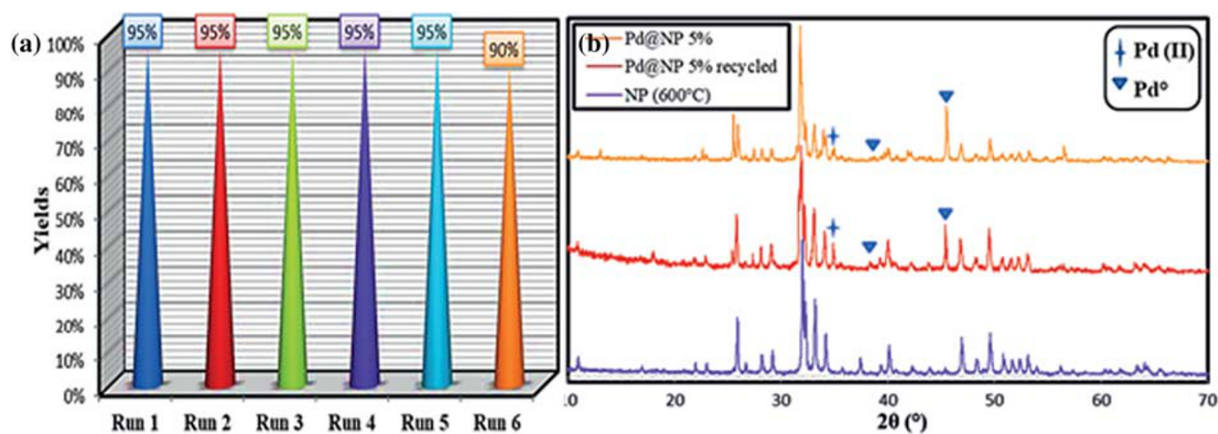
FIGURE 12 Recycling study of Pd@NP 5%: yields during recyclability (a) and X-ray diffraction (XRD) of recycled catalysts after six runs (b)
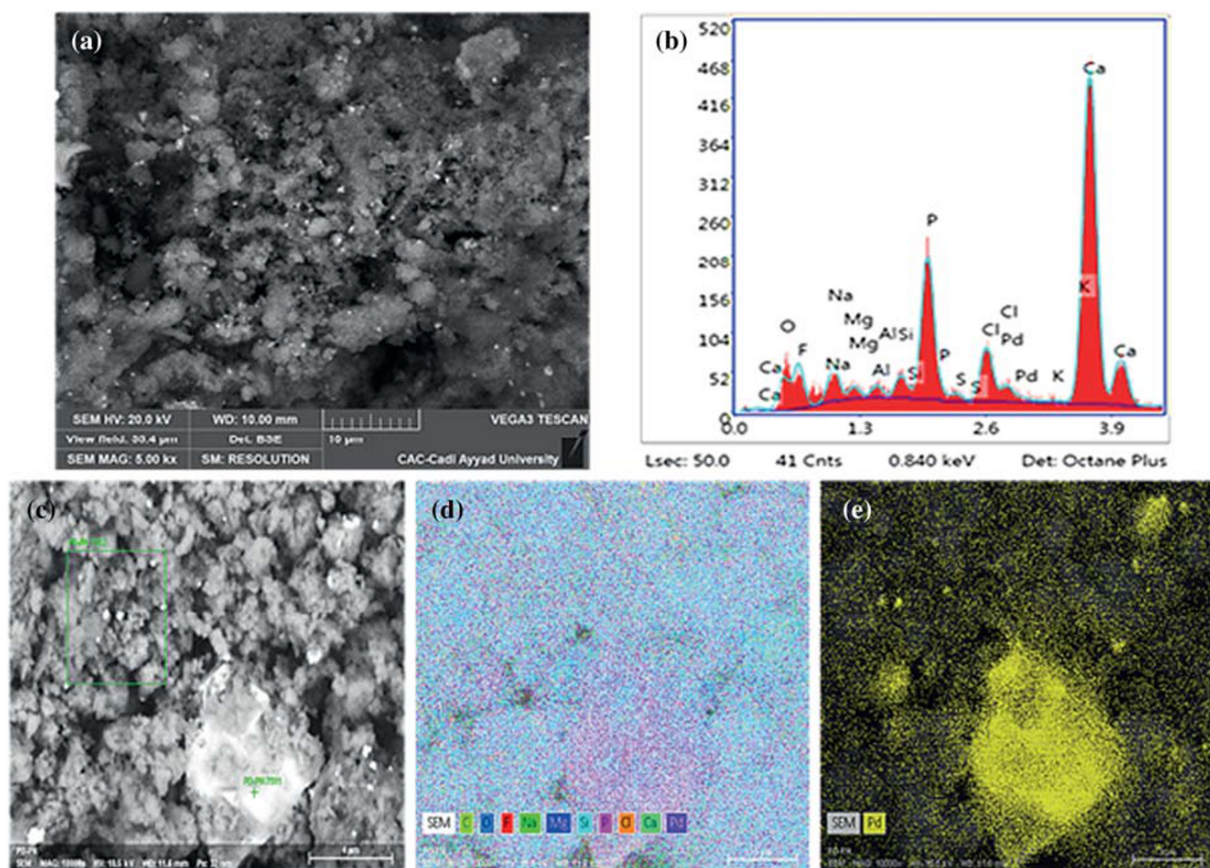
FIGURE 13 Recycling study of Pd@NP 5% catalyst: scanning electron microscopy (SEM) images and energy-dispersive X-ray (EDX) after six runs (a, b), and EDX elemental mapping analysis of recycled catalysts after six runs with (c) the studied area, (d) distribution of all elements, and (e) palladium nanoparticles distribution

8 | CONCLUSION

In summary, novel palladium nanoparticles Pd (0) with a crystallite size of 10.88 nm were synthesized and monitored by UV–Vis without using any reducing agent. The palladium nanoparticles were supported on mesoporous NP support leading to a different ratio catalyst (Pd@NP 10%, 5% and 1%). The prepared nanocatalysts were fully characterized using various analysis techniques, and their performance was first investigated in the solvent-free dehydroaromatization of himachalene mixture (*Cedrus atlantica* oil) as a model substrate before being extended to different natural terpenic olefins. The Pd@NP exhibits marked selectivity, good reusability and high stability in solvent-free dehydroaromatization of terpenes.

ORCID

Ayoub Abdelkader Mekkaoui https://orcid.org/0000-0002-7336-1961

Soufiane El Houssame https://orcid.org/0000-0003-1319-8522

REFERENCES

[1] a) B. Khodadadi, M. Bordbar, M. Nasrollahzadeh, *J. Colloid Interface Sci.* **2017**, *490*, 1; b) C. Xu, M. Nasrollahzadeh, M. Selva, Z. Issaabadi, R. Luque, *Chem. Soc. Rev.* **2019**, *48*, 4791; c) C. Xu, M. Nasrollahzadeh, M. Sajjadi, M. Maham, R. Luque, A. R. Puente-Santiago, *Renew. Sustain. Energy Rev.* **2019**, *112*, 195.

[2] a) Z. Issaabadi, M. Nasrollahzadeh, S. M. Sajadi, *J. Cleaner Prod.* **2017**, *142*, 3584; b) M. Nasrollahzadeh, S. M. Sajadi, *J. Colloid Interface Sci.* **2016**, *462*, 243; c) A. Hatamifard, M. Nasrollahzadeha, J. Lipkowski, *RSC Adv.* **2015**, *5*, 91 372.

[3] a) S. S. Momeni, M. Nasrollahzadeh, A. Rustaiyan, *J. Colloid Interface Sci.* **2017**, *499*, 93; b) T. Baran, M. Nasrollahzadeh, *Carbohydr. Polym.* **2019**, *222*, 115 029.

[4] a) M. Nasrollahzadeh, E. Mehdipour, M. Maryami, *J. Mater. Sci.: Mater. Electron.* **2018**, *29*, 17 054; b) M. Nasrollahzadeh, M. Sajjadi, J. Dadashi, H. Ghafuri, *Adv. Colloid Interface Sci.* **2020**, *276*, 102 103.

[5] F. El Aroui, S. Lahrich, A. Farahi, M. Achak, L. El Gaini, M. Bakasse, A. Bouzidi, M. A. El Mhammedi, *Electroanalysis* **2014**, *26*, 1751.

[6] A. Hassine, S. Sebti, A. Solhy, M. Zahouily, C. Len, M. N. Hedhili, A. Fihri, *Appl. Catal. Gen.* **2013**, *450*, 13.

[7] A. A. Mekkaoui, S. Jennane, A. Aberkouks, B. Boualy, A. Mehdi, M. Ait Ali, L. El Firdoussi, S. El Houssame, *Appl. Organomet. Chem.* **2019**, *33*, e5117.

[8] S. Sebti, M. Zahouily, H. Lazrek, J. Mayoral, D. Macquarrie, *Curr. Org. Chem.* **2008**, *12*, 203.

[9] a) Y. E. L. Bouabi, A. Farahi, M. Achak, M. Zeroual, K. Hnini, S. El Houssame, M. Bakasse, A. Bouzidi, M. A. El Mhammedi, J. Taiwan Inst, *Chem. Eng.* **2016**, *66*, 33; b) M. Shokouhimehr, S. M. G. Yek, M. Nasrollahzadeh, A. Kim, R. S. Varma, *Appl. Sci.* **2019**, *9*, 4183.

[10] A. Louroubi, H. Ouahine, B. Boualy, M. Ait Ali, L. El Firdoussi, *J. Adv. Catal. Sci. Technol.* **2016**, *3*, 63.

[11] *Ullmann's Encyclopedia of Industrial Chemistry*, 5th ed. Vol. A8, Willey–VCH, Weinheim **1985**, 25.

[12] D. Singh, S. M. Rao, A. K. Tripathi, *Naturwissenschaften* **1984**, *71*, 265.

[13] R. P. Adams, H. F. Linskens, J. F. Jackson (Eds), *Essential Oils and Waxes. Modern Methods of Plant Analysis*, Vol. 5, Springer **1991** 159.

[14] M. Dığrak, A. İlçim, M. Hakkı Alma, *Phyther. Res.* **1999**, *13*, 584.

[15] K. Mori, *Pure Appl. Chem.* **2001**, *73*, 601.

[16] A. Chaudhary, P. Sharma, G. Nadda, D. K. Tewary, B. Singh, *J. Insect Sci.* **2011**, *11*, 1.

[17] J.-C. Chalchat, R.-P. Garry, A. Miehet, B. Benjilali, *J. Essent. Oil Res.* **1994**, *6*, 323.

[18] R. J. Bartelt, A. A. Cossé, B. W. Zilkowski, D. Weisleder, F. A. Momany, *J. Chem. Ecol.* **2001**, *27*, 2397.

[19] K. Mori, *Tetrahedron: Asymmetry* **2005**, *16*, 685.

[20] A. Chaudhary, S. Sood, P. Das, P. Kaur, I. Mahajan, A. Gulati, B. Singh, *EXCLI j.* **2014**, *13*, 1216.

[21] K. Spielmann, R. M. De Figueiredo, J. M. Campagne, *J. Org. Chem.* **2017**, *82*, 4737.

[22] I. Hossini, M. A. Harrad, M. A. Ali, L. El Firdoussi, A. Karim, P. Valerga, M. C. Puerta, *Molecules* **2011**, *16*, 5886.

[23] R. C. Pandey, S. Dev, *Tetrahedron* **1968**, *24*, 3829.

[24] G. Mehta, S. K. Kapoor, *J. Org. Chem.* **1974**, *39*, 2618.

[25] R. J. Bartelt, D. Weisleder, F. A. Momany, *Synthesis* **2003**, *1*, 117.

[26] S. E. Muto, M. Bando, K. Mori, *Eur. J. Org. Chem.* **2004**, *2004*, 1946.

[27] S. P. Chavan, H. S. Khatod, *Tetrahedron: Asymmetry* **2012**, *23*, 1410.

[28] J. B. Bredenberg, H. Erdtman, K.-I. Persson, H. Dam, B. Sjöberg, J. Toft, *Acta Chem. Scand.* **1961**, *15*, 685.

[29] B. N. Joshi, R. Seshadri, K. K. Chakravarti, S. C. Bhattacharyya, *Tetrahedron* **1964**, *20*, 2911.

[30] T. C. Joseph, S. Dev, *Tetrahedron* **1968**, *24*, 3809.

[31] B. Abouhamza, S. Allaoud, A. Karim, *Molecules* **2001**, *6*, M236.

[32] G. H. Jimenez-Aleman, T. Schöner, A. L. Montero-Alejo, W. Brandt, W. Boland, *ARKIVOC* **2012**, *2012*, 371.

[33] G. W. Mcgraw, R. W. Hemingway, L. L. Ingram, C. S. Canady, W. B. Mcgraw, *Environ. Sci. Technol.* **1999**, *33*, 4029.

[34] D. Makarouni, S. Lycourghiotis, E. Kordouli, K. Bourikas, C. Kordulis, V. Dourtoglou, *Appl. Catal. Environ.* **2018**, *224*, 740.

[35] E. Yılmazoğlu, M. Akgün, *J. Supercrit. Fluids* **2018**, *131*, 37.

[36] A. Wróblewska, P. Miądlicki, J. Tołpa, J. Sreńsek-Nazzal, Z. C. Koren, B. Michalkiewicz, *Catalysts* **2019**, *9*, 396.

[37] C. Perego, P. Ingallina, *Catal. Today* **2002**, *73*, 3.

[38] J. Du, H. Xu, J. Shen, J. Huang, W. Shen, D. Zhao, *Appl. Catal. Gen.* **2005**, *296*, 186.

[39] M. A. Martín-Luengo, M. Yates, M. J. Martínez Domingo, B. Casal, M. Iglesias, M. Esteban, E. Ruiz-Hitzky, *Appl. Catal. Environ.* **2008**, *81*, 218.

[40] M. A. Martin-Luengo, M. Yates, E. S. Rojo, D. Huerta Arribas, D. Aguilar, E. Ruiz Hitzky, *Appl. Catal. Gen.* **2010**, *387*, 141.

[41] M. Kamitsou, G. D. Panagiotou, K. S. Triantafyllidis, K. Bourikas, A. Lycourghiotis, C. Kordulis, *Appl. Catal. Gen.* **2014**, *474*, 224.

[42] J. Zhang, C. Zhao, *ACS Catal.* **2016**, *6*, 4512.

[43] S. Lycourghiotis, D. Makarouni, E. Kordouli, K. Bourikas, C. Kordulis, V. Dourtoglou, *Mol. Catal.* **2018**, *450*, 95.

[44] M. Retajczyk, A. Wróblewska, A. Szymańska, B. Michalkiewicz, *Clay Miner.* **2019**, *54*, 121.

[45] A. Corma, S. Iborra, A. Velty, *Chem. Rev.* **2007**, *107*, 2411.

[46] R. C. Palmer, *Ind. Eng. Chem.* **1942**, *34*, 1028.

[47] B. A. Leita, A. C. Warden, N. Burke, M. S. O'Shea, D. Trimm, *Green Chem.* **2010**, *12*, 70.

[48] P. A. Weyrich, W. F. Hölderich, *Appl. Catal. Gen.* **1997**, *158*, 145.

[49] D. Buhl, P. A. Weyrich, W. M. H. Sachtler, W. F. Hölderich, *Appl. Catal. Gen.* **1998**, *171*, 1.

[50] D. Buhl, D. M. Roberge, W. F. Hölderich, *Appl. Catal. Gen.* **1999**, *188*, 287.

[51] R. J. Grau, P. D. Zgolicz, C. Gutierrez, H. A. Taher, *J. Mol. Catal. A: Chem.* **1999**, *148*, 203.

[52] P. Benavente, F. Cárdenas-Lizana, M. A. Keane, *Cat. Com.* **2017**, *96*, 37.

[53] A. M. Doyle, S. K. Shaikhutdinov, H. J. Freund, *J. Catal.* **2004**, *223*, 444.

[54] C. Perego, S. Amarilli, A. Carati, C. Flego, C. Pazzuconi, C. Rizzo, G. Bellussi, *Micro Meso Mater.* **1999**, *27*, 345.

[55] J. Čejka, A. Krejčí, N. Žilková, J. Dědeček, J. Hanika, *Micro Meso Mater.* **2001**, *44–45*, 499.

[56] J. Čejka, A. Krejčí, N. Žilková, J. Kotrla, S. Ernst, A. Weber, *Micro Meso Mater.* **2002**, *53*, 121.

[57] M. Selvaraj, A. Pandurangan, K. Seshadri, P. Sinha, V. Krishnasamy, K. Lal, *J. Mol. Catal. A: Chem.* **2002**, *186*, 173.

[58] M. Selvaraj, A. Pandurangan, K. Seshadri, P. Sinha, K. Lal, *Appl. Catal. Gen.* **2003**, *242*, 347.

[59] Natural Phosphate (NP) Comes Khouribga Region (Morocco); It Is Readily Available (Raw or Treated) from the Centre for Studies and Research of Mineral Phosphates (CERPHOS) 37, Bd My Ismail, Casablanca, Morocco.tpins

[60] B. O. Fowler, *Inorg. Chem.* **1974**, *13*, 207.

[61] A. Aberkouks, A. A. Mekkaoui, M. Ait Ali, L. El Firdoussi, S. El Houssame, *J. Chem.* **2020**, *2020*, 1.

[62] B. Hosseini, S. M. Mirhadi, M. Mehrazin, M. Yazdanian, M. R. K. Motamedi, *Trauma Mon.* **2017**, *22*, 36   139.